Nonlinear Distortions and Compensations of DFB Laser Diode in AM–VSB Lightwave CATV Applications

Hung-Tser Lin and Yao-Huang Kao, *Member, IEEE*

***Abstract*—The nonlinear distortions of direct modulated laser diode applying to AM–VSB lightwave CATV systems are studied from the viewpoint of rate equations. A simple method for calculating composite second-order distortion (CSO) is proposed, which is denoted as the quasidynamic approach. The attribution of nonlinearity from fiber dispersion and laser chirping are also concerned. The dependences on the variations of parameters of rate equations are intensively investigated to figure out the dominant factor for CSO degradation. This approach explains quite well the experimental results and gives a clue of constructing the predistortion circuit with at least 10 dB improvement.**

I. Introduction

DIRECT modulation of semiconductor lasers by a RF signal had been applied to the stringent amplitude modulation vestigial side-band (AM–VSB) lightwave cable television (CATV) systems. In this application it is essential to keep the noises and distortions originated from laser nonlinearity and fiber dispersion as small as possible [1]. Three parameters of carrier to noise ratio (CNR), composite second-order (CSO), and composite triple beat (CTB) are used to assess the multichannel transmission quality. A suggestion for CSO and CTB with good picture quality should be lower than -55 and -65 dBc in trunk applications [1]. The request of large channel capacity in CATV system gives an impetus for the fabrication of laser diode with high linearity. Very often, it is highly desired to develop linearization techniques to compensate the nonlinear distortions using only one laser diode. Here, the purposes of this paper are to examine first the nonlinear distortions of the distributed feedback (DFB) laser diode and then propose a simple method for extending of the channel capacity.

Actually, an amount of papers dealing with the nonlinear distortions of laser diode have been presented [1]–[14]. The designing rules of thumb are summarized as follows. The modulation index is generally asked to be as large as possible to reduce the laser relative intensity noise (RIN) [1]. The optical power should be as large as possible to overcome the receiver noises. Those are in the aspect of CNR. On the other hand, the modulation index is limited to avoid the nonlinear distortions from resonance distortion [1], clipping effects [2]–[4], and spatial hole burning (SHB) [5]–[9], etc. The resonance frequency of the laser diode is suggested to be larger than 7 GHz [1], even over than 10 GHz. The dc bias is suggested to the point with vanishing second-order distortion in the light versus current (L–I) relation [10]. The optimal condition of coupling constant κL between the grating and the active region of DFB laser diode has been indicated to be near to unity [11]. In the mean time, some linearization techniques such as feedforward compensation [13], selective harmonic compensation [14], and predistortion [1], [6], [7] are proposed. As a matter of fact, the last one is preferred because of using only one laser diode. In this technique, a compensated signal, which is equal in amplitude and opposite in sign to the unwanted signal produced by laser, is generated and is combined with the original signals before injecting into the laser diode. The issue is that generating such a wide band signal is a challenge work. Our approach is to generate the compensated signal within a crucial band, selected after analysis of the nonlinear nature of the laser diode. Consequently, the difficulty of circuit construction within a restricted band is reduced and good performance of at least 10 dB improvement is obtained.

To our knowledge there are two approaches in evaluating the nonlinear distortions of laser diodes in multichannel transmission. The first is to predict the CSO and CTB by directly multiplying the respective intermodulation products (IMP) to the second and third harmonic distortion evaluated from the L–I curve under the specific frequency plans and is denoted as static approach [10], [15]. These predictions ignore the frequency dependence and are applicable only in low frequency region. The second is to estimate the CSO and CTB by multiplying IMP factor to the second and third harmonic distortion derived from the rate equations [5]–[7], [16]. This approach is denoted here as quasidynamic approach. And the effect of fiber dispersion, SHB, and differential gain on nonlinearity has been discussed [5], [7]. In this paper, the quasidynamic approach is used in cooperation with a different treatment in the gain-compression term in rate equations to obtain an accurate prediction of CSO in laser diode. The analytic results of CSO after fiber dispersion are also obtained and are verified by numerical computation and are compared

Manuscript received October 17, 1995; revised July 8, 1996. This work was supported by the National Science Council, Republic of China, under Contract Number NSC84-2215-E-009-038.

The authors are with the Department of Communication Engineering and the Center of Telecommunication Research, National Chiao-Tung University, Hsin-Chu, Taiwan 30050, Republic of China.

Publisher Item Identifier S 0733-8724(96)07653-0.

with others [7], [15]. These efforts enable us to develop the predistortion circuit. Although CSO and CTB are concerned in typical CATV system, CTB is of no importance in our case and only CSO is focused [5].

The paper is organized as follows. The quasidynamic approach for CSO is presented in Section II. The procedures of parameters extraction of rate equations are also detailed. The measured and calculated nonlinear distortions are given in Section III. The dependences of parameters on distortion are also presented, from which the optimal operating point can be chosen to meet the CNR of system. The methodology of constructing the linearization circuit is also illustrated in the section. The concluding remarks are given in the last section.

II. Laser Diode and Rate Equations

A. Rate Equations and Parameters Extraction

The single-mode rate equations containing the nonlinear gain suppression factor are often employed to investigate the dynamic distortions. The variation of optical phase is also taken into account for the chirp induced distortion in the fiber. The photon density S, carrier density N and photon phase ϕ are written as [17], [18]

$$\frac{dN}{dt} = \frac{I(t)}{q\,V} - \frac{N}{\tau_e} - g_o(N - N_o)(1 - \epsilon_{\rm nl}S) \tag{1}$$

$$\frac{dS}{dt} = \Gamma g_o(N - N_o)(1 - \epsilon_{\rm nl}S) - \frac{S}{\tau_p} + \frac{\Gamma\beta N}{\tau_e} \tag{2}$$

and

$$\frac{d\phi}{dt} = \frac{1}{2}\alpha g_o(N - N_{\rm th}) \tag{3}$$

where q is the electron charge, V is the active volume, τ_e and τ_p are the respective electron and photon lifetimes, g_o is the gain constant, N_o is the carrier density for transparency, Γ is the confinement factor, β is the spontaneous emission factor, α is the linewidth enhancement factor, $N_{\rm th}$ is the carrier density at threshold as $N_{\rm th} = N_o + 1/(g_o\Gamma\tau_p)$, and $\epsilon_{\rm nl}$ is the phenomenologically nonlinear gain compression factor, and is closely related to SHB [6], [8], leakage current path [12], and lateral diffusion, etc., and results in the nonlinear L-I curve at high bias region. The driving current $I(t)$ contained dc bias and driving terms is expressed as $I(t) = I_{\rm dc} + I_{\rm ac}\sin(\omega_m t)$. The gain compression effect in rate equations is originally described as $1/\sqrt{(1 + 2\epsilon_{\rm nl}S)}$ [19] as the laser is applied in stringent lightwave CATV system and is further rewritten as $(1 - \epsilon_{\rm nl}S)$ for the case $\epsilon_{\rm nl}S \ll 1$ rather than $1/(1 + \epsilon_{\rm nl}S)$ [19]. The differences between $(1 - \epsilon_{\rm nl}S)$ and $1/(1 + \epsilon_{\rm nl}S)$ are detailed in Section III.

The laser diode studied is the Ortel 1610B DFB (distributed feedback) laser module in a 14 pin butterfly package with an internal optical isolator and thermoelectric cooler. This laser emitted at 1.3 μm is intended for CATV purpose. The values of parameters in rate equations are extracted as follows: $N_o = 1.0\times10^{24}/{\rm m}^3$ $V = 2.5\times10^{-16}$ m^3, $\Gamma = 0.3$, $g_o = 5.5\times10^{-12}$ m^3/s, $\tau_p = 1$ ps, $\tau_e = 2.988$ ns, $\beta = 2.0\times10^{-4}$, $I_{\rm th} = 21.5$ mA, and $\epsilon_{\rm nl} = 2.1\times10^{-22}$ m^3. The procedure of extraction is briefly described here. The parameters Γ, V, τ_p, and N_o closely related to the material property are from published data [17], g_o is fitted from the relation of bias current versus relaxation oscillation frequency [17], and τ_e is obtained by measuring the threshold current $I_{\rm th}$, which is expressed as $I_{\rm th} = qV(N_o + 1/(\Gamma g_o\tau_p))/\tau_e$ [17]. The spontaneous emission factor β is from fitting around the threshold of light to current curve [20]. The determination of $\epsilon_{\rm nl}$ factor is different from others [5], [17], [21]. In the previous work, the $\epsilon_{\rm nl}$ factor is found either by fitting static L-I curve [5] or by small-signal response [17], [21]. Here, in our very linear case, $\epsilon_{\rm nl}$ factor is extracted by fitting dynamically the measured CSO data as shown in Fig. 1 with all other parameters been settled. The dynamic range in our measurement set is from -70 dB due to the receiver linearity to -30 dB due to clipping. The fitted value of $\epsilon_{\rm nl}$ is 2.1×10^{-22}m^3 and is larger than that obtained from small-signal approach ($\epsilon_{\rm nl} = 6.7\times10^{-23}$). The reason is the laser diode is in large-signal operation rather than small-signal operation under multichannel transmission.

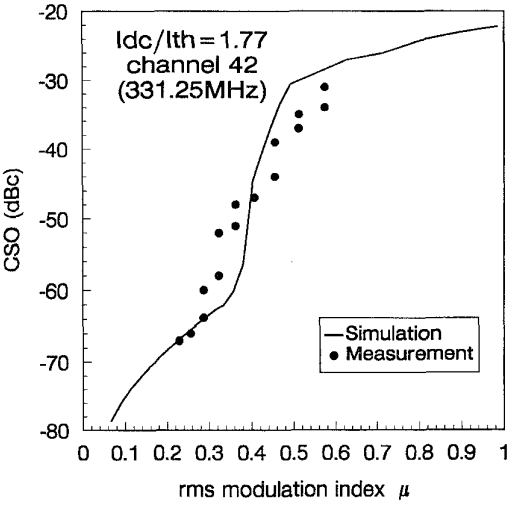

Fig. 1. The measured and calculated CSO as a function of rms modulation index with $\epsilon_{\rm nl} = 2.1\times10^{-22}$ m^3.

B. Modified Quasidynamic Approach

In order to predict rapidly the multichannel distortions, the so-called quasidynamic approach are developed again, but, with modifications in the gain compression term. First, the ratio of second harmonic distortion 2HD to fundamental C from light output $S = \bar{S} + S_1 e^{j\omega_m t} + S_2 e^{j2\omega_m t}$ of laser diode, is found as

$$\frac{\rm 2HD(2\omega_m)}{C(\omega_m)} \equiv \frac{S_2}{S_1} = \frac{C_o + C_1(j\omega_m) + C_2\omega_m^2}{D_o + D_1(j\omega_m) + D_2\omega_m^2 + D_3(j\omega_m)^3 + 4\omega_m^4} \times m \tag{4}$$

where

$$
\begin{aligned}
C_0 &= A(D + B\Gamma)(DG - EF)\\
C_1 &= A(FD + BF\Gamma + 2EF\Gamma - 2D\Gamma G)\\
C_2 &= 2AF\Gamma\\
D_0 &= (CD - BE)^2\\
D_1 &= 3(B + E)(CD - BE)\\
D_2 &= -2B^2 + 5CD - 9BE - 2E^2\\
D_3 &= 6(B + E)
\end{aligned}
$$

and

$$
\begin{aligned}
A &= \frac{(I_{\rm dc} - I_{\rm th})}{2qV}\\
B &= -g_o\bar{S}(1 - \epsilon_{\rm nl}\bar{S}) - 1/\tau_e\\
C &= -g_o(\bar{N} - N_o)(1 - 2\epsilon_{\rm nl}\bar{S})\\
D &= \Gamma(g_o\bar{S}(1 - \epsilon_{\rm nl}\bar{S}) + \beta/\tau_e)\\
E &= \Gamma g_o(\bar{N} - N_o)(1 - 2\epsilon_{\rm nl}\bar{S}) - 1/\tau_p\\
F &= -g_o(1 - 2\epsilon_{\rm nl}\bar{S})\\
G &= g_o(\bar{N} - N_o)\epsilon_{\rm nl}
\end{aligned}
$$

and modulation index m is expressed as $I_{\rm ac}/(I_{\rm dc} - I_{\rm th})$ and ω_m is rf driving frequency. The results are similar to those presented in [5, eq. (12)], but with some modifications in the expression of A to G. The distinctions are detailed in Section III.

The distortions at the far end of the fiber are then calculated. According to Meslener [22], the output optical field at the far end of the fiber is written as

$$
\begin{aligned}
e_o(t) = {} & L_o e^{j\omega_o t}\\
& + \sum_{n=1}^{\infty} + \{L_{n+} e^{j[(\omega_o + n\omega_m)t + n^2\theta_1]}\\
& \qquad + L_{n-} e^{j[(\omega_o - n\omega_m)t + n^2\theta_1]}\}
\end{aligned}
$$

where ω_o is the optical frequency and the notation L_0, L_{n+}, L_{n-}, and θ_1 are functions of amplitudes of harmonic K_0, K_1, K_2 in [22]. Here, the arguments K_0, K_1, K_2 are replaced by $\bar{S}$, S_1, and S_2, respectively. From the light intensity $|e_o(t)|^2$ the carrier C and second-order harmonic 2HD are obtained as

$$
\begin{aligned}
& C(\omega_m)\\
& = \left\{\sum_{n=0}^{\infty}[L_{n+}L_{(n+1)+} + L_{n-}L_{(n+1)-}]\cos(2n+1)\theta_1\right\}\\
& \quad \times \cos(\omega_m t)\\
& \quad - \left\{\sum_{n=0}^{\infty}[L_{n+}L_{(n+1)+} - L_{n-}L_{(n+1)-}]\sin(2n+1)\theta_1\right\}\\
& \quad \times \sin(\omega_m t)\\
& \equiv A_{\rm carrier}\cos(\omega_m t + \varphi_1), \qquad (5)
\end{aligned}
$$

$$
\begin{aligned}
& 2{\rm HD}(2\omega_m)\\
& = \left\{L_{1+}L_{1-} + \sum_{n=0}^{\infty}[L_{n+}L_{(n+2)+}\right.\\
& \qquad \left. + L_{n-}L_{(n+2)-}]\cos 4(n+1)\theta_1\right\}\cos(2\omega_m t)\\
& \quad - \left\{\sum_{n=0}^{\infty}[L_{n+}L_{(n+2)+} - L_{n-}L_{(n+2)-}]\sin 4(n+1)\theta_1\right\}\\
& \quad \times \sin(2\omega_m t)\\
& \equiv A_{\rm 2hd}\cos(2\omega_m t + \varphi_2) \qquad (6)
\end{aligned}
$$

and then the second harmonic distortion is given as $2{\rm HD}(2\omega_m)/C(\omega_m) = A_{\rm 2hd}/A_{\rm carrier}$. Moreover, it is indicated that each component attributed to CSO is equal to the secord-order intermodulation distortion (ID2) obtained by two-tone ω_i and ω_j test and thus, CSO can be expressed as the product of IMP and ID2 as ${\rm CSO}_k \cong 10\log_{10}[{\rm IMP}_k({\rm ID2}(\omega_i + \omega_j))^2]$ where the subscripts i, j and k are denoted the ith, jth and kth channel, respectively. According to Helms [16], ID2 is just twice the $2{\rm HD}/C$, i.e., ${\rm ID2}(\omega_k) = 2 \times 2{\rm HD}(\omega_k)/C(\omega_k/2)$. In addition, after further checking the (4), we confirm that $2{\rm HD}/C$ is almost linear proportional to rf driving frequency ω_k in the interested band. Hence, ${\rm ID2}(\omega_k) \cong 2{\rm HD}(2\omega_k)/C(\omega_k)$, and the expression of ${\rm CSO}_k$ can be further approximated as

$$
{\rm CSO}_k \cong 10\log_{10}[{\rm IMP}_k(2{\rm HD}(2\omega_k)/C(\omega_k))^2]. \qquad (7)
$$

The results of (7) are verified by numerical computation. For numerical purposes, (1)–(3) are further normalized by defining the normalized photon and carrier density $p = S/S_o$ and $n_c = N/N_{\rm th}$, respectively, with constant $S_o = \Gamma(\tau_p/\tau_e)N_{\rm th}$ [23]. Then the rate equations become

$$
\frac{dp}{dt} = \frac{1}{\tau_p}\left[\frac{(n_c - \delta)p(1 - \epsilon p)}{(1 - \delta)} - p + \beta n_c\right], \qquad (8)
$$

$$
\frac{dn_c}{dt} = \frac{1}{\tau_e}\left[\frac{I}{I_{\rm th}} - n_c - \frac{(n_c - \delta)p(1 - \epsilon p)}{(1 - \delta)}\right], \qquad (9)
$$

$$
\frac{d\phi}{dt} = \frac{\alpha}{2\tau_p}\left(\frac{n_c - \delta}{1 - \delta} - 1\right) \qquad (10)
$$

where the constants $\delta = N_o/N_{\rm th}$ and $\epsilon = \epsilon_{\rm nl}S_o$. The light outputs are directly calculated from (8) to (10) with the fourth-order Runge–Kutta algorithm. The current injected into the laser diode is expressed as $I(t) = I_{\rm dc} + \sum_{k=1}^{X} I_{\rm ack}\sin(2\pi f_{m,k}t + \theta_k)$, where X is the total channel numbers, $f_{m,k}$ is the kth channel frequency, θ_k is a random variable with uniform distribution, and $I_{\rm ack}$ is the amplitude of the kth channel modulation current. Here, the amplitudes are equal among the channels for testing purpose. The effective injection current appears as a Gaussian distribution with the rms modulation index μ equal to $m_k\sqrt{X/2}$, where $m_k = I_{\rm ack}/(I_{\rm dc} - I_{\rm th})$ as the channel number X is large [2]. The output of optical signal through fiber are normally treated as the following procedure. Assume that the field

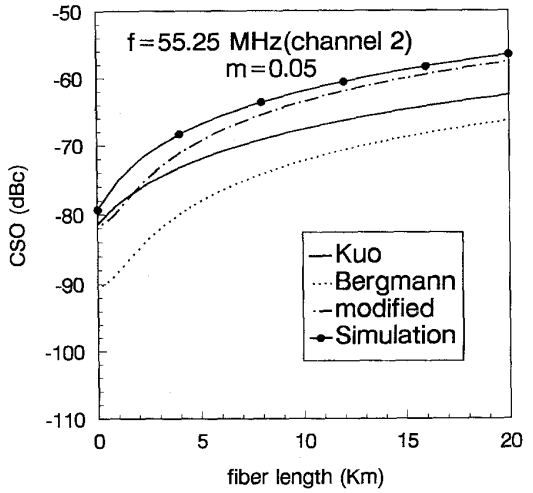

Fig. 2. The comparisons of CSO among Kuo's, Bergmann's, analytic, and numerical computation. The diode parameters are from Ortel 1610B module.

amplitude of laser light input to the fiber is expressed as $E_{\rm in}(t) = \sqrt{p}e^{j\phi}$, then the output optical field $E_{\rm out}(t)$ at the far end of the fiber is given by [24]

$$E_{\rm out}(t) = \int_{-\infty}^{\infty} \hat{E}_{\rm in}(f)H(f)e^{-j2\pi ft}df \qquad (11)$$

where $\hat{E}_{\rm in}(f) = \int_{-\infty}^{\infty} E_{\rm in}(t)e^{-j2\pi ft}dt$ are the Fourier transforms of $E_{\rm in}(t)$ and the transfer function of single mode optical fiber could be expressed as $H(f) = e^{-j\kappa_c f^2}$ with $\kappa_c = \pi D(\lambda)\lambda^2 L/c$. $D(\lambda)$ is the chromatic dispersion factor, λ is the operating wavelength and L is the fiber length. The output photocurrent is proportional to the light intensity $|E_{\rm out}(t)|^2$ from which the distortions are able to be evaluated. In executing the FFT, the time step is chosen to $\Delta t = 1.5259 \times 10^{-11}$ and 2^{18} points are concerned. In order to reduce the computer time, the down sampling method is used with sampling factor of 2, which gives rise to the total points equal 2^{17} and the resolution equal 0.25 MHz in the power spectrum analysis. The output spectra are further averaged over 25 samples for improving the accuracy.

III. Results

In this section the comparisons between the analytic results from (4) to (7) and numerical calculations from (8) to (11) are presented. How the parameters of rate equations affecting the linearity of system is indicated and then the construction of predistortion circuit is illustrated.

A. Comparison Among Kuo's [7], Bergmann's [15], and Modified Results

It is already known that CSO is degraded as the increase of modulation frequency and fiber length [7], whereas, the results are still fragmentary. Here, the comparisons among our analytic results of (7), [7, eq. (20)], [15, eq. (10)], and the numerical results are illustrated to verify the feasibility

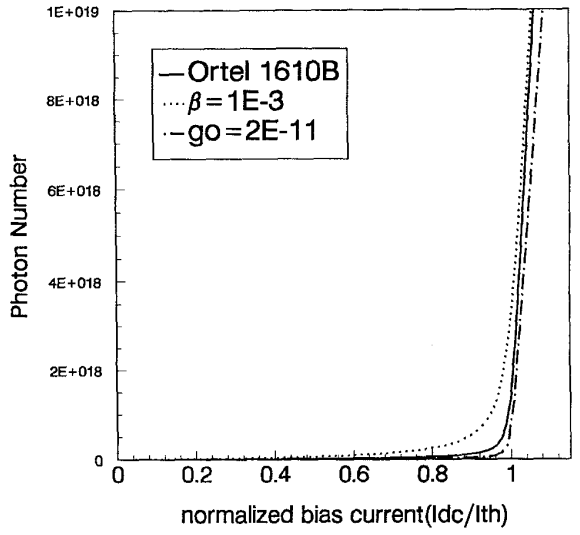

(a)

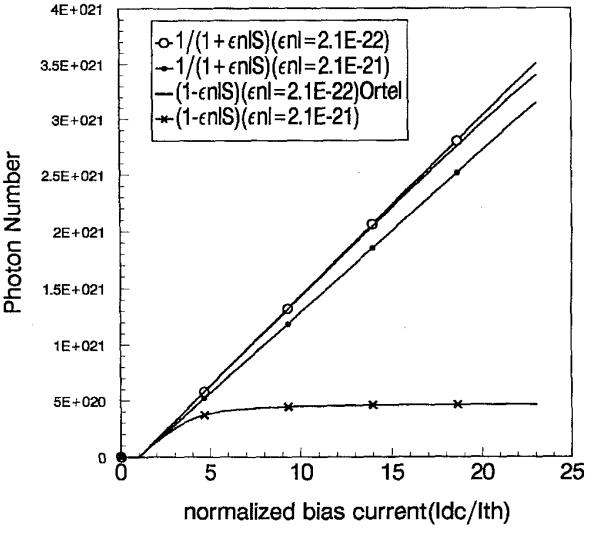

(b)

Fig. 3. The dependence of L–I curve on parameters: (a) near the threshold region and (b) high bias region.

of quasidynamic approach. The results are shown in Fig. 2 with dc bias $I_{\rm dc} = 1.5I_{\rm th}$, modulation index $m = 0.05$, and fiber dispersion coefficient $D = 17$ ps/nm · km for 42 channel transmission. Our results from (7) seem to be better than others. This is because all the Bessel functions for fiber dispersion are taken into account. In addition, the nonlinear distortions induced by intrinsic laser are also included. Thus, our approach is preferable for further investigation.

B. Dependences of CSO and L–I Curve on Parameters g_o, β, and $\epsilon_{\rm nl}$

At low frequency operation, the nonlinearity can be qualitatively predicted from the straightness of L-I curve, which, in turn, is strongly affected by three intrinsic parameters β, g_o, and $\epsilon_{\rm nl}$. Generally, β and g_o affect the threshold

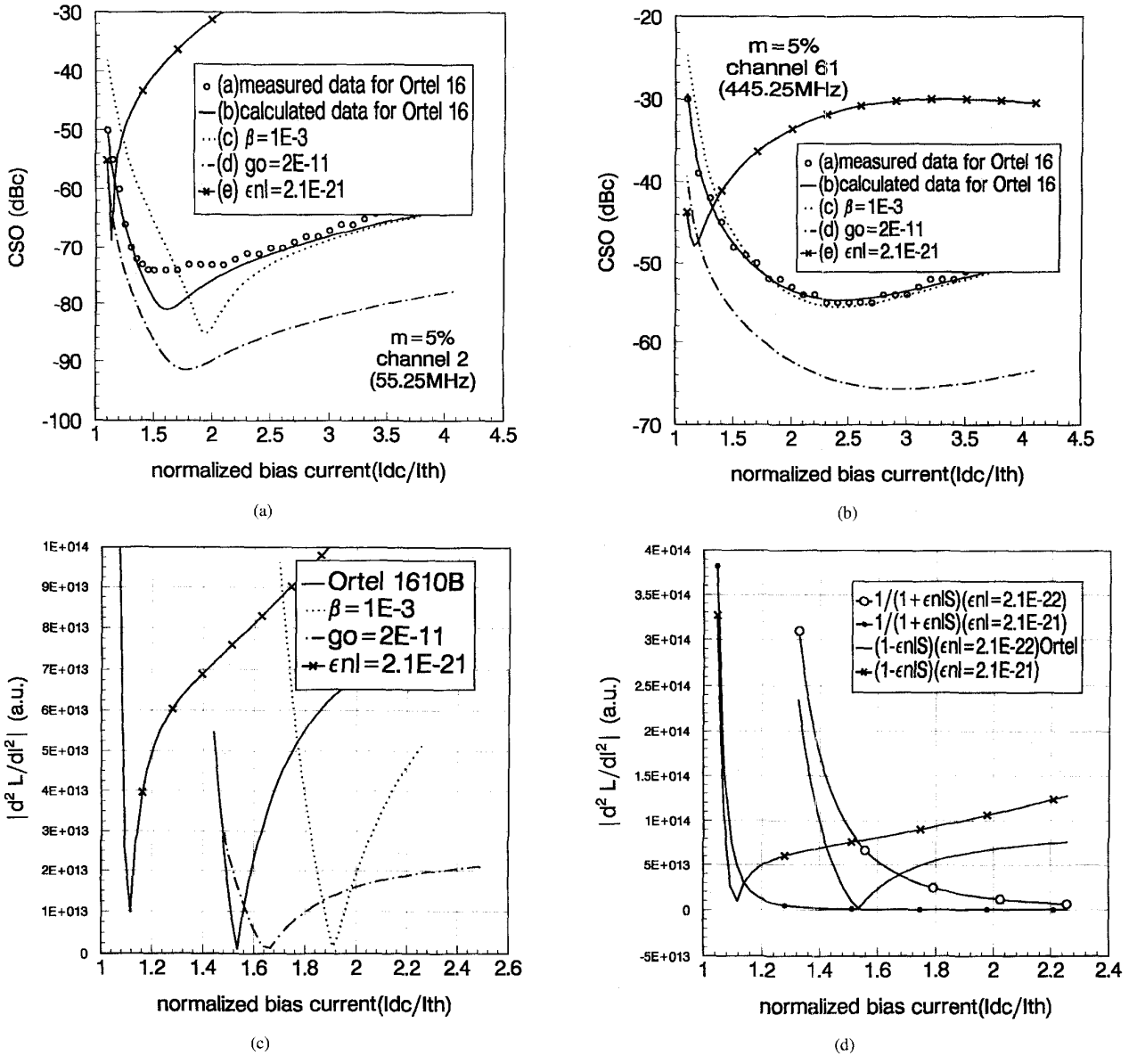

Fig. 4. CSO versus normalized bias current with various parameters at (a) channel 2 and (b) channel 61 calculated from (5). (c) and (d) are the curves of $|d^2L/dI^2|$ versus normalized bias current with the same conditions of Fig. 3(a) and (b) from static calculation.

region and $\epsilon_{\rm nl}$ affects the high current region. The typical orders of parameters β, g_o and $\epsilon_{\rm nl}$ for end-emitted laser, and quantum-well laser are around $10^{-3}\sim10^{-4}$, $10^{-11}\sim10^{-12}$ and $10^{-21}\sim10^{-23}$, respectively. CSO as functions of bias current under various combinations of orders in β, g_o, and $\epsilon_{\rm nl}$ are shown in Figs. 3 and 4 by calculated from (7). The solid line in Fig. 3(a) is the L–I curve corresponding to Ortel diode with $\beta = 2 \times 10^{-4}$, $g_o = 5.5 \times 10^{-12}$ m^3/s, and $\epsilon_{\rm nl} = 2.1 \times 10^{-22}$ m^3. The curvature around threshold becomes smooth as β is increased to 1×10^{-3} with other parameters fixed (dotted line). The reason is the spontaneous emission becomes strong and postpones the process of the stimulated emission [20]. While, the L-I curve is more sharper around threshold as g_o is increased (broken line). This is because the much larger gain g_o is, the more photon has in stimulated emission. The deterioration of straightness at high bias region from $\epsilon_{\rm nl}$ factor is detailed in Fig. 3(b). The expression of $(1 - \epsilon_{\rm nl}S)$ results in significant bending in the L-I curve. Whereas, only a slight deviation is observed for the expression of $1/(1 + \epsilon_{\rm nl}S)$ and is not for the real case. Here, the former one is chosen in this paper.

The measured CSO as a function of normalized bias current $(I_{\rm dc}/I_{\rm th})$ at lowest (channel 2) and highest (channel 61) channels are shown in Fig. 4(a) and (b), respectively. The calculated results from (7) are also shown (solid line). The calculated data match well to measured ones for both channels. The optimal bias point (dip) are near 1.61 $I_{\rm dc}/I_{\rm th}$ and 2.42 $I_{\rm dc}/I_{\rm th}$ at channel 2 and 61, respectively, for Ortel 1610B.

The slight deviation around the minimum point for channel 2 in Fig. 4(a) is due to the limitation of receiver linearity. The effects of parameters variations are also examined as curves (c), (d) and (e) in Fig. 4(a) and (b). The dips shift due to the movement of inflection point in L-I curve. If the L-I relation is expressed as $L = L_o + L_1(I - I_{\rm dc}) + L_2(I - I_{\rm dc})^2 + \cdots$, where L is the photon density, $I_{\rm dc}$ is the dc bias, L_o, L_1 and L_2 are the constant and depend on the selection of $I_{\rm dc}$; then, the optimal bias with minimum CSO is at $|d^2L/dI^2| = 0$ (i.e., $L_2 = 0$). $|d^2L/dI^2|$ as a function of bias are shown in Fig. 4(c) for various β, g_o and $\epsilon_{\rm nl}$ factor. The optimal bias points are almost matching to the points in Fig. 4(a) of low frequency channel. The optimal points in curve b, c, d, and e of Fig. 4(a) are 1.61, 1.95, 1.75, and 1.15 $I_{\rm dc}/I_{\rm th}$, and the relative points in Fig. 4(c) are 1.54, 1.9, 1.7, and 1.12 $I_{\rm dc}/I_{\rm th}$. While, these results are different from those at high frequency channel [see Fig. 4(b)]. It implies that static approach is useful only in low frequency region. Besides that, the dynamic features regarding to the parameters are summarized as follows: As the g_o factor is raised, the relaxation oscillation frequency is lifted far above CATV band and leads to ultra low distortion as shown in curve (d) of Fig. 4(a) and (b). CSO is degraded with large gain compression factor $\epsilon_{\rm nl}$ as shown in curve (e) of Fig. 4(a) and (b) and $\epsilon_{\rm nl}$ is the crucial factor for nonlinear distortion. Again, no dips are found for the case of $(1/1 + \epsilon_{\rm nl}S)$ as shown in Fig. 4(d). Thus, the expression of $(1/1 + \epsilon_{\rm nl}S)$ is not suitable for the real situation as compared to the experimental results.

C. Predistortion Technique

As indicated in Fig. 4, the proper setting of dc bias near dip is essential to minimize the CSO and, thus, leads the construction of the predistortion circuit in an easier way. To obtain a global picture, the frequency dependences of CSO at various bias from (7) are shown in Fig. 5 with parts of measured results also indicated (square dot). CSO is over -60 dBc at high frequency region. Here, bias point at $I_{\rm dc} = 2.79I_{\rm th}$ (60 mA) is chosen for the reason of larger output power and larger CNR, rather than at $I_{\rm dc} = 2I_{\rm th}$ with better CSO only. A small fraction of CSO at high frequency band from 330 to 450 MHz is over the specification and needs to be ameliorate. Because CSO is closely related to 2HD as stated above the distortion can be improved only treating the signal within frequency band from 165 to 225 MHz with $m = 0.18$. Fortunately, from (4), the frequency-dependence of 2HD/C reveals the form of $(a + bf_m) + j(c - df_m)$ with negligible secord-order terms under low modulation index where f_m (MHz) is the driving frequency. In our case, the terms $a(= 4.14\times10^{-4})$, bf_m $(= -2.05\times10^{-6}f_m)$, and $c(= 1.2\times10^{-4})$ are smaller than $-jdf_m(= -j3.64 \times 10^{-6}f_m)$ for f_m in the frequency range from 165 to 225 MHz. Further investigation shows that the last term $-jdf_m$ plays an important role in reducing 2HD/C to an acceptable level. This one-term correction can simplify the construction of circuit.

As mentioned, the function of predistortion circuit is to generate a compensated signal which is equal in amplitude and opposite in sign to that produced by laser. The block diagram of the predistorter is proposed in Fig. 6. The injected rf signal

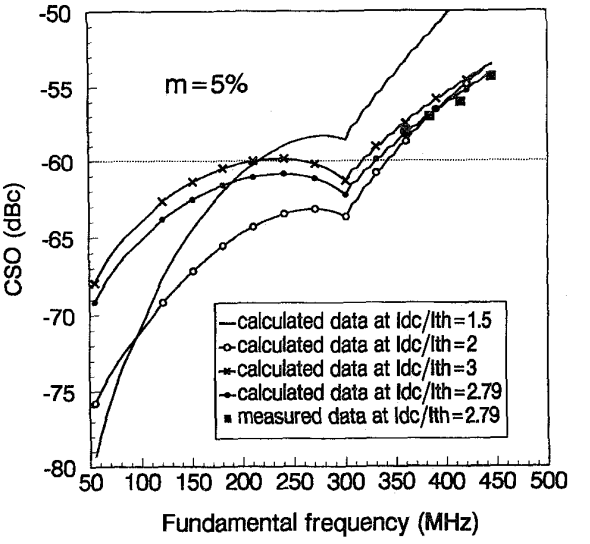

Fig. 5. CSO as functions of driving frequency at various dc bias currents.

is split into two parts, one is directly into the combiner and the other is fed into the predistortion circuit, which consist of squarer, tunable attenuator, and frequency-dependent circuit, to generate distorted signal $-jdf_m$. The magnitude of each block is calibrated by a single-tone testing. For example, at 180 MHz, the second harmonic is approximately -65 dBc under large 18% modulation index as shown in Fig. 7(a) which is nearly equal to the calculated one $(20 \times \log(3.64 \times 10^{-6} \times 180) = -63.67$ dBc). The splitter and combiner consist of ferrite-based broadband directional coupler with 15 dB tapping. The squarer circuit is the active mixer with -5 dB conversion loss, and the tunable attenuator has enough dynamical range (40 dB) and bandwidth to set the amplitude of compensated signal. The phase delay consists of a section of coaxial cable about 10 cm in length to trim the phase different between two paths. The frequency dependent element is a 1 pF capacitance in series connection to provide jf_m term and about 13 dB insertion loss at 180 MHz. The group delay of the components in the predistortion route are negligible. After compensation, the second harmonic of the laser output is down to -84 dBc as shown in Fig. 7(b). With such a single-tone calibration, CSO in multichannel transmission is significantly improved. For convenience, CSO and CTB as functions of frequency are shown in Fig. 8. With the predistorter, CSO are 10 dB down, and CTB are almost unchanged. It is noted that this method can be extended for ultra-wideband improvement by separating the deteriorated band into several bands with their own phase and attenuation factors. As for CTB improvement, a similar way is suggested to generate third order term to cancel the third order distortion, although it is not necessary in our case.

IV. Conclusion

In this article, the distortion and compensation of the single-mode DFB laser with applications to AM–VSB lightwave CATV systems are discussed. The nonlinear behaviors are precisely predicted by the proposed quasidynamic approach with

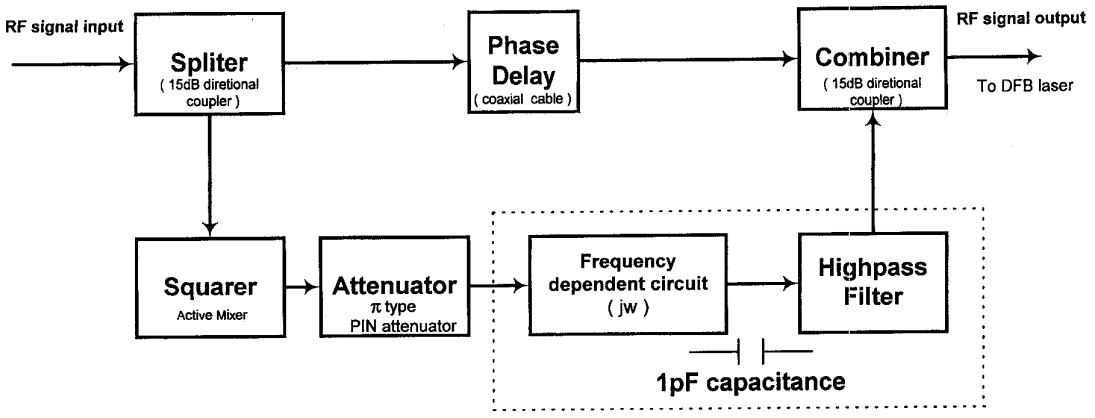

Fig. 6. The block diagram of the predistortion circuit.

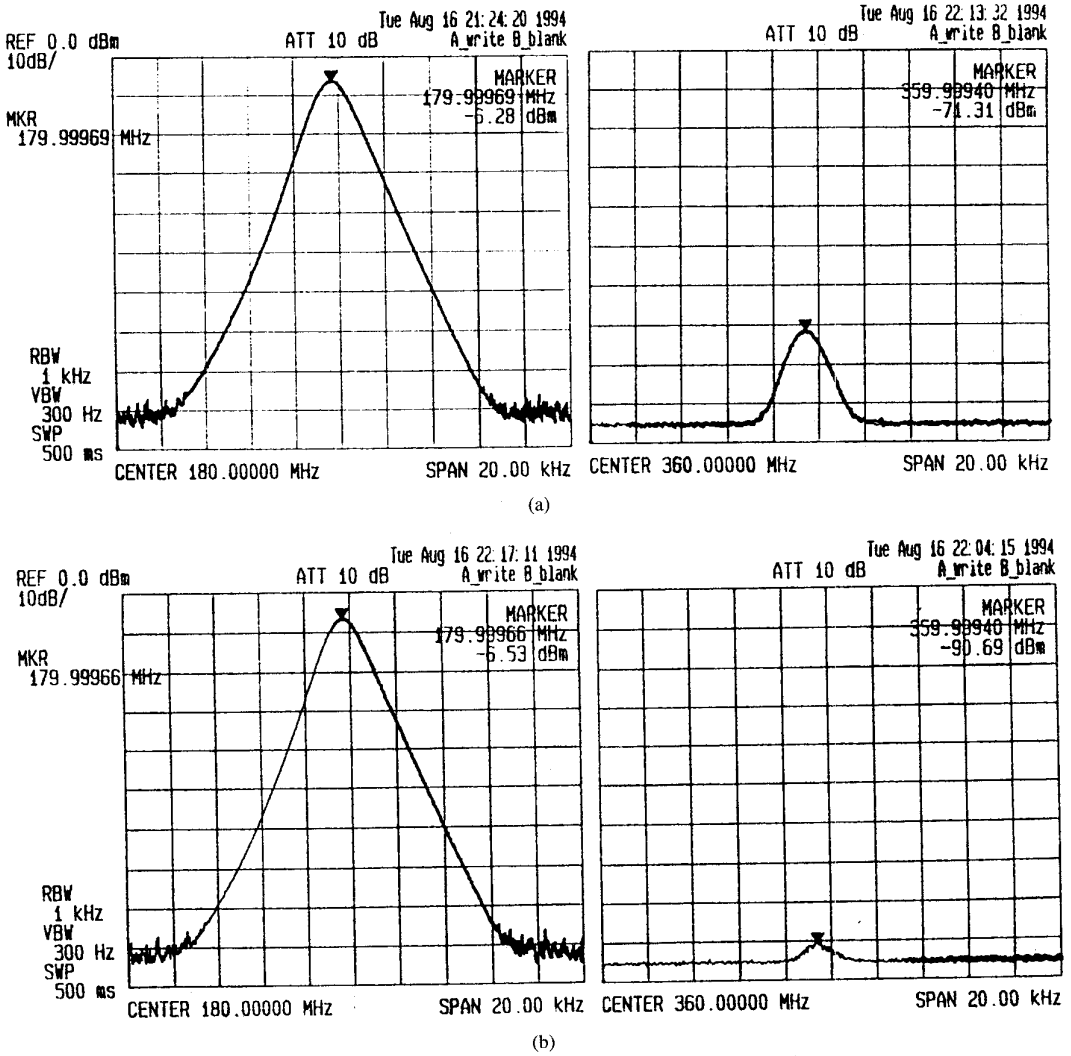

Fig. 7. The second harmonic distortion under single-tone test at 180 MHz with $m = 18\%$. (a) -65 dBc without and (b) -84 dBc with predistortion circuit.

special care in gain compression factor. It is deduced that the setting of bias point is crucial for the low distortion operation. The second harmonic distortion is able to be approximated by a linearly frequency dependent term, which results in a simple construction of predistortion circuit. With appropriate selection of bias and predistortion circuit, the channel capacity extension from 42 channel (up to 330 MHz) to 60 channel (up to 450 MHz) is demonstrated. Our results provide as a

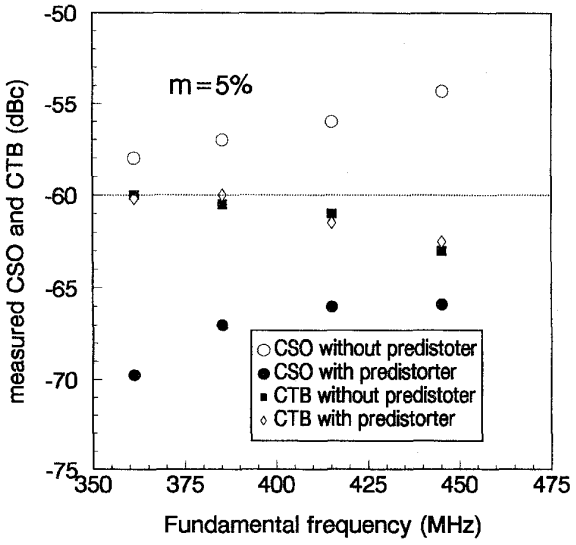

Fig. 8. CSO and CTB as functions of frequency at with and without predistortion circuit presented.

guideline for improving the linearity of the laser diodes for AM-VSB lightwave system.

ACKNOWLEDGMENT

The authors would like to thank Prof. W. I. Way for his encouragement during the development of predistorter and J.-H. Hsu for his computer calculations.

REFERENCES

[1] T. E. Darcie and G. E. Bodeep, "Lightwave subcarrier CATV transmission systems," *IEEE Trans. Microwave Theory Tech.*, vol. MTT-38, pp. 524–533, May 1990.
[2] A. A. M. Saleh, "Fundamental limit on number of channels in subcarrier-multiplexed lightwave CATV system," *Electron. Lett.*, vol. 25, no. 12, pp. 776–777, June 1989.
[3] C. J. Chung and I. Jacobs, "Simulation of the effects of laser clipping on the performance of AM SCM lightwave systems," *IEEE Photon. Technol. Lett.*, vol. 3, pp. 1034–1036, Nov. 1991.
[4] M. R. Phillips and T. E. Darcie, "Numerical simulation of clipping-induced distortion in analog lightwave systems," *IEEE Photon. Tech. Lett.*, vol. 3, no. 12, pp. 1153–1155, 1991.
[5] C. Y. Kuo, "Fundamental second order nonlinear distortions in analog AM CATV transport systems based on single frequency semiconductor lasers," *J. Lightwave Technol.*, vol. 10, pp. 235–243, Feb. 1992.
[6] C. Y. Kuo and E. E. Bergmann, "Second-order distortion and electronic compensation in analog links containing fiber amplifiers," *J. Lightwave Technol.*, vol. 10, pp. 1751–1759, Nov. 1992.
[7] C. Y. Kuo, "Fundamental nonlinear distortions in analog links with fiber amplifiers," *J. Lightwave Technol.*, vol. 11, pp. 7–15, Jan. 1993.
[8] R. H. Wentworth, "Large-scale longitudinal spatial-hole-burning contribution to laser gain compression," *IEEE J. Quantum Electron.*, vol. 29, no. 7, pp. 2145–2153, July 1993.
[9] G. Motthier, "Influence of the carrier density dependence of the absorption on the harmonic distortion in semiconductor lasers," *J. Lightwave Technol.*, vol. 11, pp. 16–19, Jan. 1993.
[10] J. Lipson et al., "High-fidelity lightwave transmission of multiple AM-VSB NTSC signals," *IEEE Trans. Microwave Theory Tech.*, vol. MTT-38, no. 5, pp. 483–492, May 1990.
[11] A. Takemoto et al., "Distributed feedback laser diode and module for CATV systems," *IEEE J. Select. Areas Commun.*, vol. 8, pp. 1359–1364, Sept. 1990.
[12] M. S. Lin, S. J. Wang, and N. K. Dutta, "Measurements and modeling of the harmonic distortion in InGaAsP distributed feedback lasers," *IEEE J. Quantum Electron.*, vol. 26, pp. 998–1004, June, 1990.
[13] L. Fock et al., "Reduction of semiconductor laser intensity noise by feedforward compensation: Experiment and theory," *IEEE. J. Lightwave Technol.*, vol. 10, pp. 1919–1925, Dec. 1992.
[14] J. Straus, "Linearized transmitters for analog fiber links," *Laser Focus*, pp. 54–61, Oct. 1978.
[15] E. E. Bergmann, C. Y. Kuo, and S. Y. Huang, "Dispersion induced composite second-order distortion at 1.5 μm," *IEEE Photon. Technol. Lett.*, vol. 3, pp. 59–61, Jan. 1991.
[16] J. Helms, "Intermodulation distortions of broad-band modulated laser diodes," *J. Lightwave Technol.*, vol. 10, pp. 1901–1906, Dec. 1992.
[17] Y. H. Kao and H. T. Lin, "A study of harmonic distortions and period doubling in DFB ridge waveguide laser with strong current modulation," *Opt. Commun.*, vol. 88, pp. 415–418, 1992.
[18] J. C. Cartledge and G. S. Burley, "The effect of laser chirping on lightwave system performance," *J. Lightwave Technol.*, vol. 7, pp. 568–573, Mar. 1989.
[19] G. P. Agrawal, "Effect of gain and index nonlinearities on single-mode dynamics in semiconductor lasers," *IEEE J. Quantum Electron.*, vol. 26, pp. 1901–1909, Nov. 1990.
[20] G. P. Agrawal and N. K. Dutta, *Long-wavelength Semiconductor Lasers*. New York: Van Nostrand, 1986, p. 226.
[21] E. Hemery *et al.*, "Dynamic behaviors of semiconductor lasrs under strong sinusoidal current modulation: Modeling and experiments at 1.3 μm," *IEEE J. Quantum Electron.*, vol. 26, pp. 633–641, Apr. 1990.
[22] G. J. Meslener, "Chromatic dispersion induced distortion of modulated monochromatic light employing direct detection," *IEEE J. Quantum Electron.*, vol. 20, pp. 1208–1216, Oct. 1984.
[23] G. P. Agrawal, "Effects of gain nonlinearities on period doubling and chaos in directly modulated semiconductor lasers," *Appl. Phys. Lett.*, vol. 49, pp. 1013–1015, 1986.
[24] A. F. Elrefaire *et al.*, "Chromatic dispersion limitations in coherent lightwave transmission systems," *J. Lightwave Technol.*, vol. 6, pp. 704–709, May 1988.

Hung-Tser Lin was born in Taipei, Taiwan, R.O.C., in 1967. He received the B.S. degree from Feng-Chia University, Tai-Chung in 1989, and the M.S. and Ph.D. degrees from National Chiao-Tung University, Hsinchu, in 1991 and 1996, respectively.

His research interests include nonlinear dynamics in laser diode and optical communication systems.

Yao-Huang Kao (M'86) was born in Tainan, Taiwan, R.O.C., in 1953. He received the B.S., M.S., and Ph.D. degrees from National Chiao-Tung University in electronic engineering in 1975, 1977, and 1986, respectively.

Since 1986, he has joined the Faculty of the Department of Communication Engineering, National Chiao-Tung University, and is now a Full Professor. In 1988, he was a Visiting Scholar working in nonlinear circuit at University of California, Berkeley. His current research interests involve nonlinear dynamics and chaos, high-speed optical communications, and microwave circuit designs.